iScience

CellPress
OPEN ACCESS

Article

Self-assembly of a multimeric genomic hydrogel via multi-primed chain reaction of dual single-stranded circular plasmids for cell-free protein production

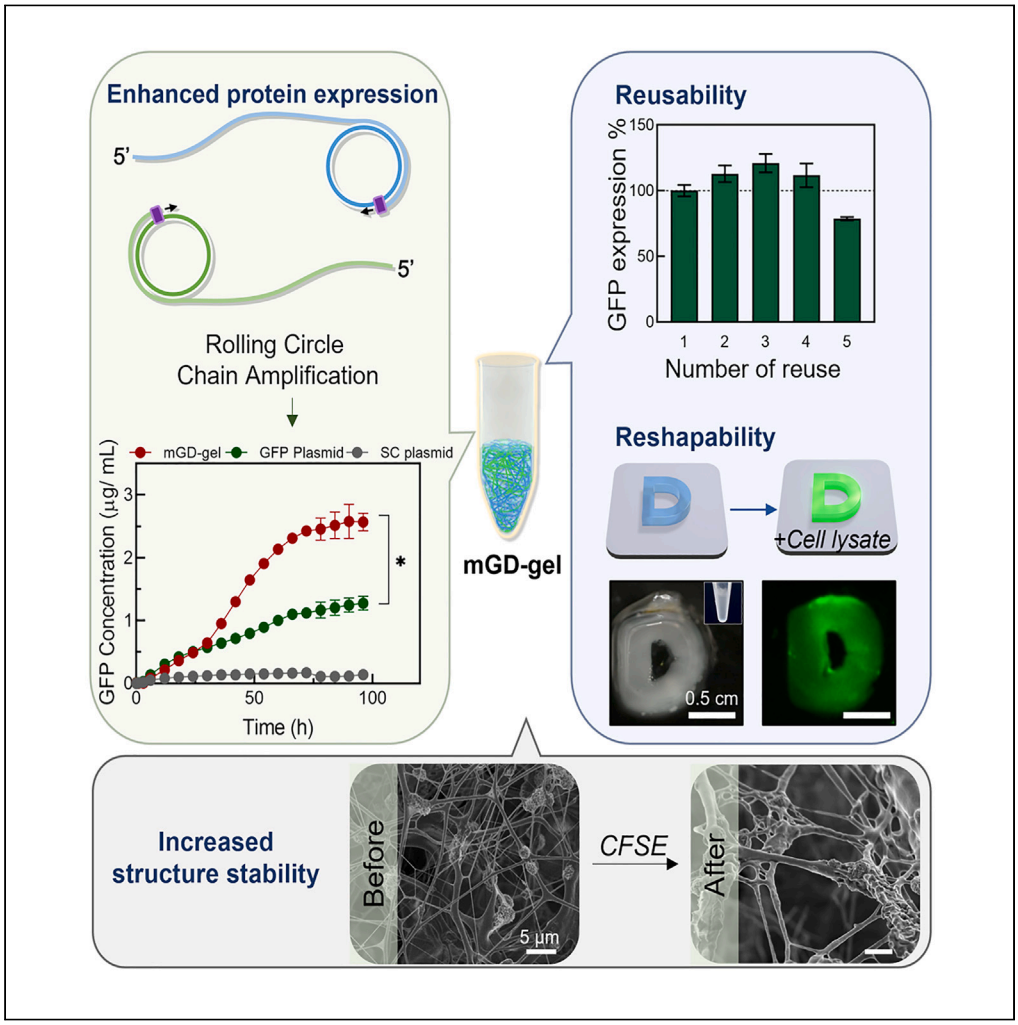

Hyangsu Nam, Taehyeon Kim, Sunghyun Moon, Yoonbin Ji, Jong Bum Lee

jblee@uos.ac.kr

Highlights

Multi-genomic hydrogels (mGD-gel) enhance protein expression efficiently

RCCA synthesizes mGD-gel using two ssDNA plasmids as templates

Stable and recyclable mGD-gel supports protein expression

Customizable mGD-gel shapes for diverse applications

Nam et al., iScience 26, 107089
July 21, 2023
https://doi.org/10.1016/j.isci.2023.107089

iScience

CellPress
OPEN ACCESS

Article

Self-assembly of a multimeric genomic hydrogel via multi-primed chain reaction of dual single-stranded circular plasmids for cell-free protein production

Hyangsu Nam,[1] Taehyeon Kim,[1] Sunghyun Moon,[1] Yoonbin Ji,[1] and Jong Bum Lee[1,2,*]

SUMMARY

Recent technical advances in cell-free protein synthesis (CFPS) offer several advantages over cell-based expression systems, including the application of cellular machinery, such as transcription and translation, in the test tube. Inspired by the advantages of CFPS, we have fabricated a multimeric genomic DNA hydrogel (mGD-gel) via rolling circle chain amplification (RCCA) using dual single-stranded circular plasmids with multiple primers. The mGD-gel exhibited significantly enhanced protein yield. In addition, mGD-gel can be reused at least five times, and the shape of the mGD-gel can be easily manipulated without losing the feasibility of protein expression. The mGD-gel platform based on the self-assembly of multimeric genomic DNA strands (mGD strands) has the potential to be used in CFPS systems for a variety of biotechnological applications.

INTRODUCTION

The production of recombinant proteins has revolutionized the field of biotechnology.[1–3] Biotechnological processes have been extensively developed for the production of recombinant therapeutic proteins. However, conventional cell-based protein production often faces certain obstacles, such as protease contamination and difficulty in cell reproduction.[4,5] In addition, cell-based gene expression is low-yielding, time-consuming, and cell-type-dependent.

Cell-free protein synthesis (CFPS) has been rapidly developed to overcome the inherent limitations of traditional protein expression methods, such as difficulties in cell preparation and limited gene expression in cells.[6] Without the hassle associated with cell manipulation, CFPS has successfully used (or replicated) the cellular machinery of life, such as transcription and translation in the test tube (or an *in situ* system).

The CFPS in the solution state has shown promise as a versatile platform for the rapid and efficient production of proteins. For example, CFPS has been used to produce a range of proteins, from simple single-domain proteins to more complex multi-domain proteins, including membrane proteins and viral capsid proteins. Additionally, CFPS has been used to produce proteins with a range of post-translational modifications, such as phosphorylation and glycosylation.[7,8] Despite these successes, CFPS in the solution state also has several limitations. One major limitation is the lack of a functional membrane environment, which can be important for the correct folding and the activity of certain membrane proteins. Another limitation is the limited scalability of CFPS in the solution state, which can make it challenging to produce large quantities of proteins.[9] Finally, the cost of the solution phase system results in a single-use gene template.[10,11]

To address this issue, hydrogels have been applied for cell-free protein production by crosslinking gene templates with synthetic molecules, such as fibroin,[12] cellulose,[13] and polyethylene glycol diacrylate (PEGDA).[11] In detail, hydrogel-based CFPS, with conventional plasmids as expression templates, has successfully achieved high-yield protein production and reusability.[14–18]

The use of a hydrogel scaffold provides a more biomimetic environment that can better mimic the *in vivo* cellular environment, which can lead to enhanced protein folding and activity.[19] Additionally, the use of a hydrogel scaffold can also improve the stability and reusability of the CFPS system, as the hydrogel can protect the protein synthesis machinery from degradation and can be easily manipulated for repeated use.[20] In particular, self-assembled DNA-based hydrogels have emerged as versatile biomaterials for efficient

[1]Department of Chemical Engineering, University of Seoul, 163 Seoulsiripdaero, Dongdaemun-gu, Seoul 02504, Republic of Korea

[2]Lead contact

*Correspondence: jblee@uos.ac.kr

https://doi.org/10.1016/j.isci.2023.107089

loading of gene templates via enzymatic self-assembly,[21–26] hybridization with sticky ends,[27] and modification of chemical linker.[28] For this reason, the Luo research group has developed a solid-phase protein production system using DNA hydrogels.[29–31] Specifically, protein-producing DNA micro-pads, a DNA microgel, and a PEGDA/DNA hybrid hydrogel with plasmids have been synthesized for reusable CFPS.[11,32]

However, the use of high-concentration plasmids as expression templates in CFPS still requires a traditional plasmid cloning step, which can be a challenge for certain proteins such as toxin proteins.[33] To address this issue, the self-assembly of hydrogels with a linear plasmid DNA template has been employed after amplification by polymerase chain reaction (PCR).[21,30,32,34–39] Compared with the preparation of a conventional plasmid expression template, linear plasmid-based CFPS can be prepared just after PCR.[40] Despite its advantages, such as simple mass production and simplicity, the linear plasmid-based system can still suffer from low reaction yields because of the open linear templates with increased vulnerability to remaining nucleases in the cell-free environment.[41,42]

Inspired by the previously developed DNA hydrogel using a rolling circle amplification technique, herein, we describe a strategy for synthesizing a multimeric genomic DNA hydrogel (mGD-gel) via self-assembly of multimeric genomic DNA strands (mGD strands) encoding multimeric genomic sequences. To achieve the self-assembly of the mGD-gel, we applied rolling circle chain amplification (RCCA) using dual single-stranded DNA circular plasmids (ssDNA plasmid). Importantly, the mGD-gel only consists of numerous tandem repeats of mGD strands produced by using RCCA from the double-stranded DNA circular plasmid (dsDNA plasmid) template. This approach allows the genomic DNA to not only create a hydrogel structure but also to become a medium for protein expression in the mGD-gel. Hence, our mGD-gel is likely to provide a new route for cell-free protein production via the self-assembly of mGD strands.

RESULTS

Design and fabrication of multimeric genomic DNA hydrogel for CFPS

To fabricate an mGD-gel for efficient and reusable CFPS, rolling circle replication[21,39,43,44] was used for the amplification of mGD strands. The amplified mGD strands were assembled through a simple one-pot process to form a hydrogel. This process utilized two complementary ssDNA plasmids templates significantly reducing the possibility of nonspecific amplification.[45,46] This process involved RCCA with two ssDNA plasmids derived from heat-denatured dsDNA plasmid (Figure 1A). Two complementary ssDNA plasmids were initially obtained from the dsDNA plasmid encoding the gene of interest (GOI), including the T7 promoter region. The ssDNA plasmids were used as templates for the RCCA process. To achieve chain reaction during rolling circle amplification, two complementary circular DNAs are necessary. The RCCA was performed using two complementary ssDNA circular plasmids. As a result, elongated mGD strands encoding multimeric GOI were produced and self-assembled through a complementary sequence between the elongated gene products. The mGD-gel composed of mGD strands encoding multimeric GOI was produced after sufficient amplification and elongation by RCCA (Figure 1B). As a proof of concept, our mGD-gel was designed to encode a GFP-expressing gene in a GFP-encoding plasmid DNA (pIDTSMART-AMP_EGFP) (Table S1) for cell-free protein expression.

Morphological analysis of the self-assembly of multimeric genomic DNA strands

Gradual time-dependent self-assembly of the mGD-gel was observed over 24 h of reaction time (Figure 2A). We have analyzed the early stages of the mGD-gel using atomic force microscopy (AFM) images. As shown in the AFM images, the amplified mGD strands were cross-linked to form network structures. The generation of mGD strands was observed after 30 min RCCA reaction. The amplified mGD strands began to become entangled after 2 h and more entanglement was observed after 6 h. Interestingly, particularized entanglement of mGD strands was observed after 12 h, indicating stable crosslinking of the mGD strands. After further crosslinking and self-assembly, a premature mGD-gel was synthesized. The topographical 3D images showed increased thickness at the 24 h time point compared to the early reaction time (Figure 2B). The line profiles were also measured after 30 min and 24 h of RCCA reaction, revealing an increase in the thickness of the network structure, thereby demonstrating the formation of the crosslinked structure of mGD strands.

To confirm the gelation process, the optical density (OD) of the DNA network was measured at 600 nm over the gelation reaction duration (Figure 2C). In addition, to assess the necessity of RCCA for mGD-gel formation, the OD of the precursor hydrogel solution, including template ssDNA plasmids with primer 1 only,

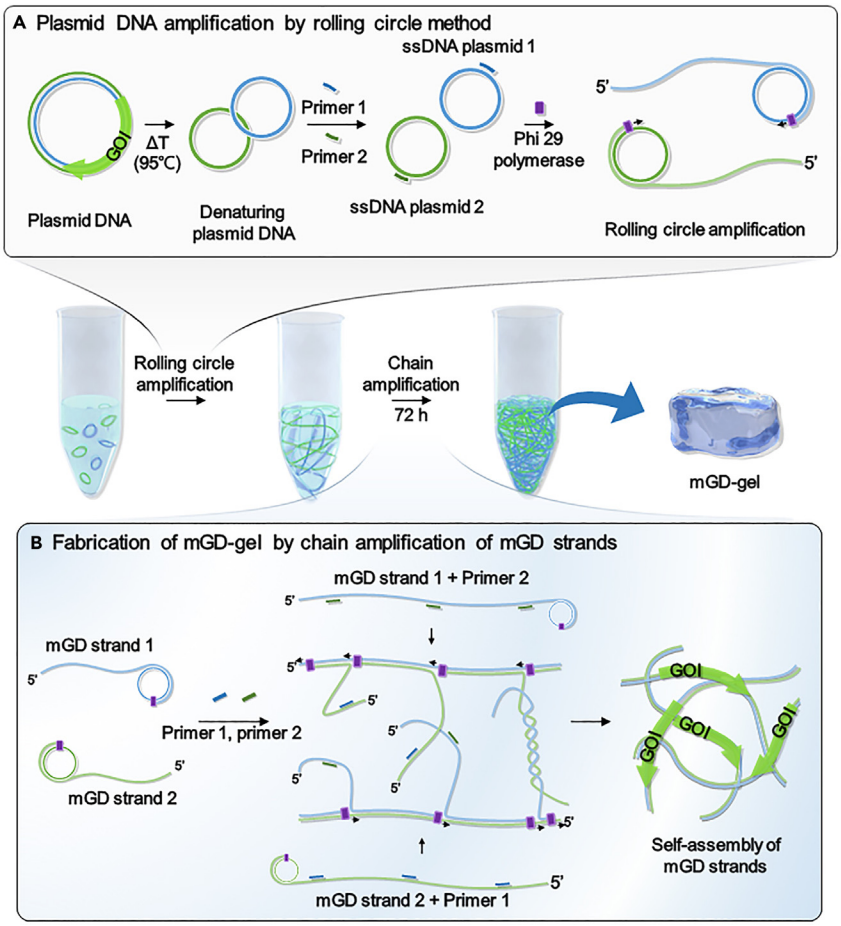

Figure 1. Illustration depicting the fabrication of the multimeric genomic DNA hydrogel (mGD-gel)

(A) A synthetic method based on the rolling circle amplification reaction from single-stranded DNA circulars.

(B) Self-assembled mGD-strands diagram depicting the formation of mGD-gel by rolling circle chain amplification (RCCA) from single-strand circulars and mechanism of cell-free reaction in cell lysate.

template ssDNA plasmids with primer 2, ssDNA plasmids with primers 1 and 2 (precursor solution of mGD-gel), or scramble ssDNA plasmids with primers 1 and 2, were further analyzed. When only primer 1 or 2 was added to the precursor solution, the OD value did not increase as significantly as that of the precursor mGD-gel solution, indicating the importance of chain amplification for successful gelation. In the control group, rolling circle amplification from only one template ssDNA plasmid was performed without the chain reaction. The successful formation of mGD-gel was confirmed by SEM images showing dense network structures after 72 h of reaction (Figure 2D). High-magnification images showed approximately 100–200 nm thick strings as building blocks made of multimeric genomic DNA in a stable gel structure. The increased roughness of the surface morphology indicated the formation of dense networks in the mGD-gel (Figure 2E).

Cell-free protein production and reusability of mGD-gel

To evaluate protein expression in mGD-gels containing tandem repeats of GFP-encoding sequences in the cell-free system, GFP production was analyzed by real-time PCR (RT-PCR). As the fluorescence intensity increases in proportion to the initial number of template DNA molecules in RT-PCR,[47] the mGD-gel could also generate strong fluorescent intensity, indicating efficient protein production. As shown in the inset fluorescence images in Figure 3A, the fluorescence image of the mGD-gel after 48 h of cell-free reaction was significantly brighter than that of the other control groups. Additionally, it was confirmed that the mGD-gel showed high amplification efficiency of the mGD strands containing 15282 μg of GFP-encoding sequence through RCCA (Table S3). To analyze the amount of GFP produced, the intensity value was

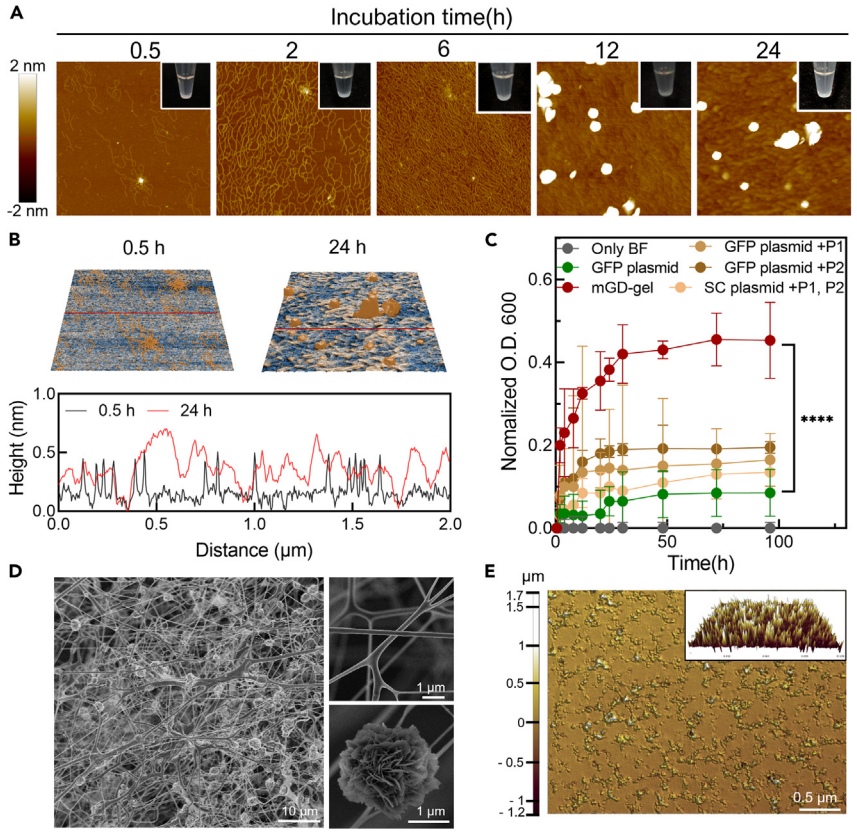

Figure 2. Morphology of the mGD-gel

(A) Time-dependent AFM analysis of morphological polymerization in early stages. The mGD-strands digital image of polymerization product over time (inset).

(B) 3D images reveal the presence of the hydrogel surface at 0.5 h and 24 h. At the bottom, the gray profile corresponds to the red line drawn over 0.5 h, and the red profile is the surface roughness corresponding to the red line drawn over 24 h.

(C) BF, plasmids, scrambled plasmids containing primers 1 and 2, plasmids incubated with each primer, and optical density (OD) values at each time point of the mGD-gel.

(D and E) SEM image and (E) non-contact 3D surface profiler surface roughness analysis of mGD-gel. Inset image shows a 3D image of a non-contact 3D surface profiler. (p value was assigned by one-way ANOVA with Dunnett's post-hoc test (****$p < 0.0001$).

converted according to the calibration curve construction standard and analyzed as a graph (Figure 3B). The protein yield from the mGD-gel expressed at approximately 2.57 μg/mL was 2.5-fold higher than that of the GFP plasmid.

To confirm the efficiency of CFPS, mRNA levels were analyzed using mGD-gel, GFP plasmid, scramble plasmid (SC plasmid), and the negative control (no template control, NTC) based on the invasion signal amplification reaction with the GFP primer (Figure 3C). In target amplification, the reactions containing the mGD-gel showed an increase in fluorescence within only seven cycles from the start reaction, corresponding to the fluorescence result presented in Figure 3A. Based on the results shown in Figure 3C, the concentration of mRNA was analyzed as a cycle threshold (Ct) value, which represents the number of cycles required to amplify RNA to reach a significant level during RT-qPCR. Low Ct values are associated with increased efficiency of protein expression because Ct values have an inverse relationship with the mRNA load. In Figure 3D, the GFP gene has been presented on the mGD-gel at low Ct values, indicating a high concentration of GFP mRNA. In addition, GFP expressed on the mGD-gel exhibited a 2-fold higher mRNA production efficiency than that of the normal plasmid solutions. Additionally, we also analyzed the level of luminance in the luciferase gene encoded mGD-gel (Luc-mGD-gel) and compared it with control groups (Figure S1). Luc-mGD-gel showed 5119.49 RLU, while Luc plasmid and SC plasmid showed 3363.25 RLU and 213.357 RLU, respectively. As a result, it was also confirmed that the Luc-mGD-gel encoding

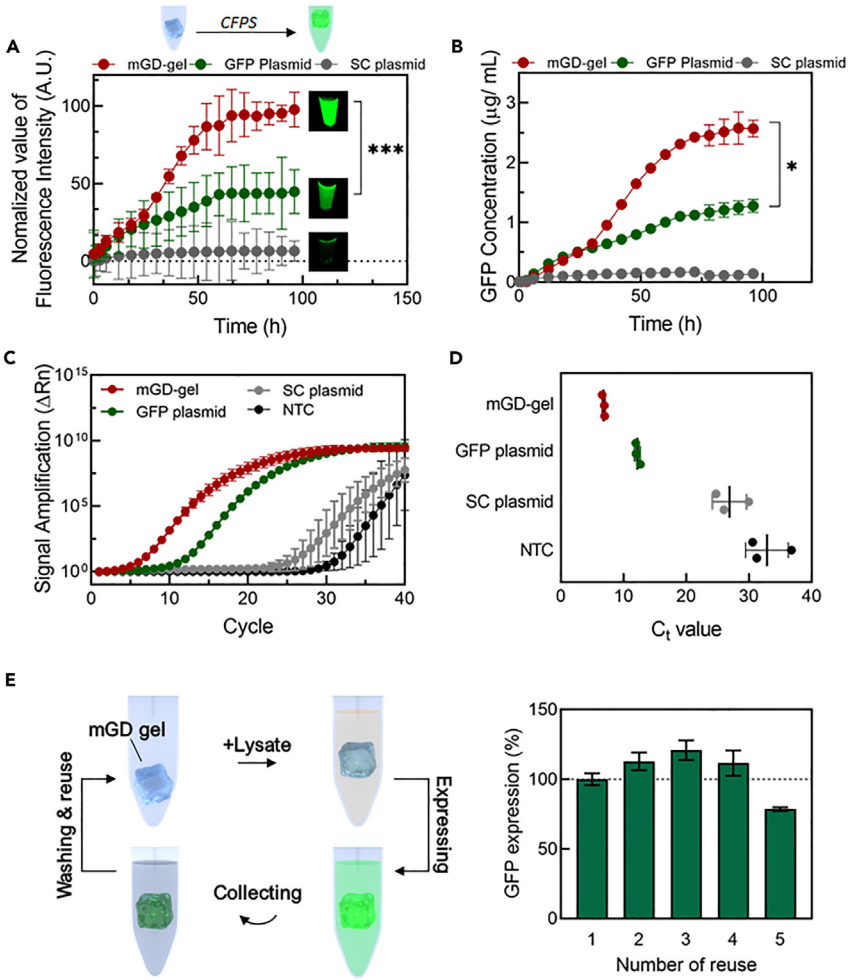

Figure 3. Transcription and GFP expression kinetic of CFPS reactions

(A) Effect of mGD-gel on GFP translation in a cell-free system.

(B) Comparison of expression yield of GFP of mGD-gel to an SC plasmid and GFP plasmid solution control.

(C–E) qRT-PCR amplification plots and (D) Ct values of RNA samples extracted from mGD-gel (red) or GFP plasmid (green) (E) Scheme depicting the reuse process of mGD-gel and reuse of an mGD-gel in GFP expression. (p value was assigned by one-way ANOVA with Dunnett's post-hoc test [*$p < 0.05$, **$p < 0.01$, ***$p < 0.001$]).

luciferase was expressed more effectively in the gel form than in the general solution state. This is the same, and it can be seen that the mGD strands were effectively elongated by the RCCA synthesis method. These results indicate that the mGD-gel provides a high concentration of exposed protein expression sites and can be effectively used as a material for cell-free protein expression. These results indicate that the mGD-gel offers an efficient approach to cell-free protein expression for various genes, enabling stable and continuous protein production.

Importantly, the mGD-gel not only expressed proteins very efficiently but was also reusable despite being constructed based on DNA. As shown in Figure 3E, the mGD-gel could be used for GFP protein expression five times. Interestingly, it was observed that the expression rates during the second and third protein production were slightly higher than those during the primary protein production because the assembled structure could slightly loosen over time, thereby increasing the chances of efficient protein expression. Subsequently, it was observed that the protein expression level decreased by more than 3-fold, but the mGD-gel remained reusable. To confirm the successful formation and structural stability of the mGD-gel, SEM analysis was performed after the CFPS reaction. The results of our analysis reveal that the mGD-gel maintains a dense network structure, characterized by the formation of particles and thin strands,

which closely resemble its pre-reaction state. These observations suggest that the mGD-gel retains its structural integrity and stability, even after undergoing protein expression (Figure S2). The energy dispersive spectroscopy (EDS) analysis results showed a significant increase in nitrogen (N) and oxygen (O) levels for the mGD-gel after CFPS than before CFPS, indicating potential evidence of RNA and protein expression in the gels (Figure S3).[48] Specifically, the mGD-gel exhibited N and O levels of 5.10% and 30.72%, respectively, before CFPS, which increased to 12.35% and 39.25%, respectively, after CFPS. These findings demonstrate the efficacy of mGD-gels in supporting the transcription of RNA into proteins, suggesting its potential for protein expression. Taken together, the ability of mGD-gels to maintain their structural integrity even after protein expression further supports its promising candidacy for such applications.

The mGD-gel, synthesized through self-assembly technique using mGD strands, has the potential to preserve and reutilize DNA templates in CFPS and showed promising results in terms of elevated protein yields.

Reshaping and CFPS of mGD-gel

The mGD-gel can be reshaped into various shapes through simple molding techniques, as demonstrated in Figure 4. To achieve this, we utilized a freeze-casting approach to induce the reconstruction of the internal structure of mGD-gel. This technique increases the local concentration of DNA while also allowing nucleic acids to maintain and enhance their function in the frozen state.[49] Consequently, we were able to improve the stability and reshaping properties of self-assembled mGD strands in this system.

In Figure 4A, the D-shape mGD-gel is produced by using a master mold for casting the reshaped mGD-gel. After freezing for 24 h, the reshaped mGD-gel was successfully achieved from the PDMS molds (Figure 4B). The extracted mGD-gel was stained with DNA-specific dye, GelRed, confirming again the incorporation of DNA within the reshaped gel (Figure S4A). After reshaping the mGD-gel, its mechanical and viscoelastic properties were analyzed to confirm gel formation (Figures 4C, 4D, and S4B). Interestingly, the storage modulus (G′) and loss modulus (G") of the analyzed mGD-gel exhibited more stable viscoelasticity in strain-dependence than reshaped mGD-gel (Figure 4C). However, frequency-dependent oscillatory rheological measurement showed that reshaped mGD-gel had higher tensile properties than original mGD-gel (Figure 4D). The results showed the storage modulus (G′) and loss modulus (G″), indicating that the freeze-casting method was suitable for reshaping the mGD-gel while maintaining the gel properties. In addition, the mechanical robustness of the reshaped mGD-gel could be improved using this method.

To verify the functionality of mGD-gel after reshaping, mGD-gel was reshaped as a D shape and performed GFP expression in the cell-free system (Figure 4E). The fluorescence image at the bottom of Figure 4E shows the successful expression of the GFP protein. The reshaped mGD-gel was incubated for 48 h with cell lysis, and the GFP intensity increased to 32%. This indicates that the reshaping of mGD-gel maintained cell-free protein productivity. These results suggest that reshaping mGD-gel is versatile and easily fabricable, providing an effective platform for CFPS. Collectively, reshaping mGD-gel offers advantages in terms of easy handling and stability. Its changed three-dimensional structure provides a stable microenvironment for protein synthesis and expressed protein. Additionally, the ability to reshape mGD-gel into different forms and sizes provides the potential for customization and versatility in various applications, offering advantages in terms of easy handling, stability, and reusability for efficient protein expression.

DISCUSSION

In summary, we have developed the mGD-gel based on the self-assembly of mGD strands. The mGD strands were successfully generated from dual ssDNA plasmid templates by RCCA. The CFPS was a one-pot process when using the mGD-gel. Our CFPS system is the most noteworthy in terms of enhancing the protein expression from a plasmid hydrogel platform with mGD-gel, which is composed of only tandem repeats of linear plasmids, termed mGD strands. In this system, the challenge of CFPS research was to improve the efficiency, yield, and quality of protein production while reducing costs. In addition, the flexible mechanical properties of the mGD-gel allowed it to be reshaped and injected into a customized mold. Taking advantage of the mGD-gel, CFPS can be applied to proteins required for local and long-term expression. In addition, the RCCA process ensures stable protein expression by increasing the long-term genetic stability of the mGD strands amplified from the dual ssDNA plasmid templates. Considering this advantage, the system described herein has the potential to be a universal synthesis method for

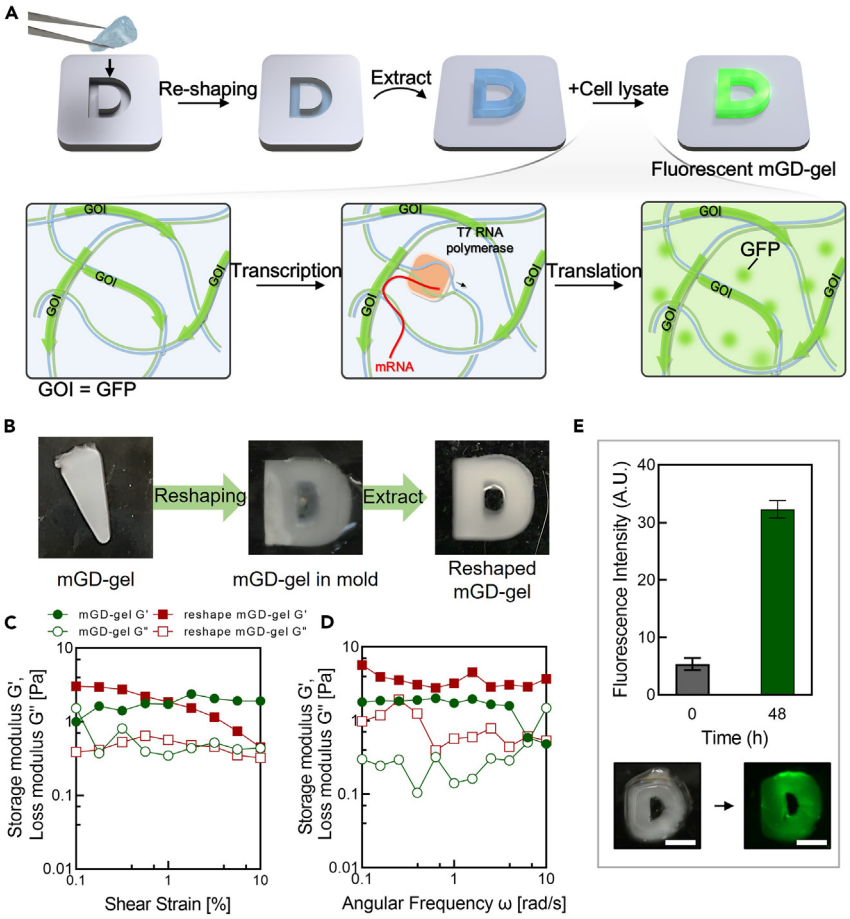

Figure 4. Reshaping of mGD-gel

(A) Schematic illustration of manufacturing the reshaping mGD-gel and CFPS reaction on the reshaping mGD-gel.

(B) Digital images of the process of manufactured reshaping mGD-gel.

(C and D) Mechanical properties of mGD-gel and reshaping mGD-gel. Strain-stress curves and angular frequency-dependent (ϵ = 1%, 25°C) storage (G′) and loss (G″) modulus.

(E) Green protein expression intensity over time in reshaping mGD-gel encoding GFP. The digital images below the graph were captured before CFPS reshaping mGD-gel (left) and after CFPS reshaping mGD-gel (right). Reshaping mGD-gel (left) and after CFPS reshaping mGD-gel (right). Scale bar: 0.5 cm.

protein expression without considering the cellular environment, which is critical for translation. The mGD-gel's reusability, moldability, and injectability hold promise as functional genetic materials for diverse biomedical and biotechnology applications. Further advancements in this research field will require optimizing reaction conditions, exploring cell-free systems for various genes, and utilizing advanced technologies such as microfluidics and automation to enhance protein synthesis capabilities.

Limitations of the study

This study aimed to evaluate the efficacy of mGD-gel in the expression of green fluorescent and luciferase proteins. Our findings demonstrated that the mGD-gel exhibited superior protein expression compared to the plasmid solution. In order to improve protein synthesis efficiency using the RCCA method in future studies, further research is needed to explore more diverse plasmid designs.

STAR★ METHODS

Detailed methods are provided in the online version of this paper and include the following:

- KEY RESOURCES TABLE

SUPPLEMENTAL INFORMATION

Supplemental information can be found online at https://doi.org/10.1016/j.isci.2023.107089.

ACKNOWLEDGMENTS

This work was supported by the Creative Materials Discovery Program through the National Research Foundation of Korea (NRF) funded by the Ministry of Science and ICT (MSIT) [grant number NRF-2017M3D1A1039423], [2022R1A2C2004820], and [2022M3E5F1081326]. Commercialization Promotion Agency for R&D Outcomes (COMPA) funded by the MSIT [grant number 1711149621].

AUTHOR CONTRIBUTIONS

H.N. and J.B.L. were responsible for the study's conceptualization and design. T.K. conducted the AFM analysis and produced a PDMS mold for the mGD-gel shaping process. S.M. carried out the mRNA-level analysis of the mGD-gel, while Y.J. designed the graphical representation. H.N. and J.B.L. wrote the article. All authors reviewed and contributed to the final manuscript.

DECLARATION OF INTERESTS

The authors declare no competing interests.

INCLUSION AND DIVERSITY

We support the inclusive, diverse, and equitable conduct of research.

Received: January 27, 2023
Revised: April 20, 2023
Accepted: June 7, 2023
Published: June 10, 2023

REFERENCES

1. Nobeli, I., Favia, A.D., and Thornton, J.M. (2009). Protein promiscuity and its implications for biotechnology. Nat. Biotechnol. *27*, 157–167. https://doi.org/10.1038/nbt1519.

2. Niemeyer, C.M. (2001). Nanoparticles, proteins, and nucleic acids: biotechnology meets materials science. Angew Chem. Int. Ed. Engl. *40*, 4128–4158. https://doi.org/10.1002/1521-3773(20011119)40:22<4128::AID-ANIE4128>3.0.CO;2-S.

3. Otto, T., and Sicinski, P. (2017). Cell cycle proteins as promising targets in cancer therapy. Nat. Rev. Cancer *17*, 93–115. https://doi.org/10.1038/nrc.2016.138.

4. Jo, D., Liu, D., Yao, S., Collins, R.D., and Hawiger, J. (2005). Intracellular protein therapy with SOCS3 inhibits inflammation and apoptosis. Nat. Med. *11*, 892–898. https://doi.org/10.1038/nm1269.

5. Dimitrov, D.S.J.T.P. (2012). Therapeutic Proteins, pp. 1–26.

6. Li, J., Liu, H., Wang, C., and Huang, G. (2017). A facile method to fabricate hybrid hydrogels with mechanical toughness using a novel multifunctional cross-linker. RSC Adv. *7*, 35311–35319. https://doi.org/10.1039/c7ra05645a.

7. Hershewe, J.M., Warfel, K.F., Iyer, S.M., Peruzzi, J.A., Sullivan, C.J., Roth, E.W., DeLisa, M.P., Kamat, N.P., and Jewett, M.C. (2021). Improving cell-free glycoprotein synthesis by characterizing and enriching native membrane vesicles. Nat. Commun. *12*, 2363. https://doi.org/10.1038/s41467-021-22329-3.

8. Oza, J.P., Aerni, H.R., Pirman, N.L., Barber, K.W., ter Haar, C.M., Rogulina, S., Amrofell, M.B., Isaacs, F.J., Rinehart, J., and Jewett, M.C. (2015). Robust production of recombinant phosphoproteins using cell-free protein synthesis. Nat. Commun. *6*, 8168. https://doi.org/10.1038/ncomms9168.

9. Kwon, Y.-C., and Jewett, M.C. (2015). High-throughput preparation methods of crude extract for robust cell-free protein synthesis. Sci. Rep. *5*, 8663. https://doi.org/10.1038/srep08663.

10. Park, N., Kahn, J.S., Rice, E.J., Hartman, M.R., Funabashi, H., Xu, J., Um, S.H., and Luo, D. (2009). High-yield cell-free protein production from P-gel. Nat. Protoc. *4*, 1759–1770. https://doi.org/10.1038/nprot.2009.174.

11. Cui, J., Wu, D., Sun, Q., Yang, X., Wang, D., Zhuang, M., Zhang, Y., Gan, M., and Luo, D. (2020). A PEGDA/DNA hybrid hydrogel for cell-free protein synthesis. Front. Chem. *8*, ARTN.28. https://doi.org/10.3389/fchem.2020.00028.

12. Lee, M.S., Hung, C.S., Phillips, D.A., Buck, C.C., Gupta, M.K., and Lux, M.W. (2020). Silk fibroin as an additive for cell-free protein synthesis. Synth. Syst. Biotechnol. *5*, 145–154. https://doi.org/10.1016/j.synbio.2020.06.004.

13. Ullah, M.W., Ul-Islam, M., Khan, S., Kim, Y., and Park, J.K. (2015). Innovative production of bio-cellulose using a cell-free system derived from a single cell line. Carbohydr. Polym. *132*, 286–294. https://doi.org/10.1016/j.carbpol.2015.06.037.

14. Guzman-Chavez, F., Arce, A., Adhikari, A., Vadhin, S., Pedroza-Garcia, J.A., Gandini, C., Ajioka, J.W., Molloy, J., Sanchez-Nieto, S., Varner, J.D., et al. (2022). Constructing cell-free expression systems for low-cost access. ACS Synth. Biol. *11*, 1114–1128. https://doi.org/10.1021/acssynbio.1c00342.

15. Benítez-Mateos, A.I., Zeballos, N., Comino, N., Moreno de Redrojo, L., Randelovic, T., and López-Gallego, F. (2020). Microcompartmentalized cell-free protein synthesis in hydrogel mu-channels. ACS Synth. Biol. *9*, 2971–2978. https://doi.org/10.1021/acssynbio.0c00462.

16. Kim, J.S., Choi, J.S., and Cho, Y.W. (2017). Cell-free hydrogel system based on a tissue-specific extracellular matrix for in situ adipose tissue regeneration. Acs Appl Mater Inter *9*, 8581–8588. https://doi.org/10.1021/acsami.6b16783.

17. Benítez-Mateos, A.I., Zeballos, N., Comino, N., Moreno de Redrojo, L., Randelovic, T., and López-Gallego, F. (2020). Microcompartmentalized cell-free protein synthesis in hydrogel μ-channels. ACS Synth. Biol. *9*, 2971–2978.

18. Kim, J.S., Choi, J.S., Cho, Y.W., and interfaces. (2017). Cell-free hydrogel system based on a tissue-specific extracellular matrix for in situ adipose tissue regeneration. ACS Appl. Mater. Interfaces *9*, 8581–8588.

19. Sun, Z.Z., Yeung, E., Hayes, C.A., Noireaux, V., and Murray, R.M. (2014). Linear DNA for rapid prototyping of synthetic biological circuits in an Escherichia coli based TX-TL cell-free system. ACS Synth. Biol. *3*, 387–397. https://doi.org/10.1021/sb400131a.

20. Pardee, K., Green, A.A., Ferrante, T., Cameron, D.E., DaleyKeyser, A., Yin, P., and Collins, J.J. (2014). Paper-based synthetic gene networks. Cell *159*, 940–954. https://doi.org/10.1016/j.cell.2014.10.004.

21. Lee, J.B., Peng, S., Yang, D., Roh, Y.H., Funabashi, H., Park, N., Rice, E.J., Chen, L., Long, R., Wu, M., and Luo, D. (2012). A mechanical metamaterial made from a DNA hydrogel. Nat. Nanotechnol. *7*, 816–820. https://doi.org/10.1038/nnano.2012.211.

22. Nam, H., Jeon, H., Kim, H., Yoon, H.Y., Kim, S.H., and Lee, J.B. (2023). Module-assembly of injectable cellular DNA hydrogel via clickable cells and DNA scaffolds. Chem. Eng. J. *452*, 139492. https://doi.org/10.1016/j.cej.2022.139492.

23. Han, S., Park, Y., Kim, H., Nam, H., Ko, O., and Lee, J.B. (2020). Double controlled release of therapeutic RNA modules through injectable DNA-RNA hybrid hydrogel. ACS Appl. Mater. Interfaces *12*, 55554–55563. https://doi.org/10.1021/acsami.0c12506.

24. Um, S.H., Lee, J.B., Park, N., Kwon, S.Y., Umbach, C.C., and Luo, D. (2006). Enzyme-catalysed assembly of DNA hydrogel. Nat. Mater. *5*, 797–801. https://doi.org/10.1038/nmat1741.

25. Lee, J.B., Peng, S., Yang, D., Roh, Y.H., Funabashi, H., Park, N., Rice, E.J., Chen, L., Long, R., Wu, M., and Luo, D. (2012). A mechanical metamaterial made from a DNA hydrogel. Nat. Nanotechnol. *7*, 816–820.

26. Nam, H., Jeon, H., Kim, H., Yoon, H.Y., Kim, S.H., and Lee, J.B. (2023). Module-assembly of injectable cellular DNA hydrogel via clickable cells and DNA scaffolds. Chem. Eng. J. *452*, 139492.

27. Zhou, X., Li, C., Shao, Y., Chen, C., Yang, Z., and Liu, D. (2016). Reversibly tuning the mechanical properties of a DNA hydrogel by a DNA nanomotor. Chem. Commun. *52*, 10668–10671. https://doi.org/10.1039/c6cc04724f.

28. Jahanban-Esfahlan, R., Seidi, K., Jahanban-Esfahlan, A., Jaymand, M., Alizadeh, E., Majdi, H., Najjar, R., Javaheri, T., and Zare, P. (2019). Static DNA nanostructures for cancer theranostics: recent progress in design and applications. Nanotechnol. Sci. Appl. *12*, 25–46. https://doi.org/10.2147/Nsa.S227193.

29. Ruiz, R.C., Kiatwuthinon, P., Kahn, J.S., Roh, Y.H., and Luo, D. (2012). Cell-free protein expression from DNA-based hydrogel (P-gel) droplets for scale-up production. Ind. Biotechnol. *8*, 372–377. https://doi.org/10.1089/ind.2012.0024.

30. Kahn, J.S., Ruiz, R.C.H., Sureka, S., Peng, S., Derrien, T.L., An, D., and Luo, D. (2016). DNA microgels as a platform for cell-free protein expression and display. Biomacromolecules *17*, 2019–2026. https://doi.org/10.1021/acs.biomac.6b00183.

31. Ruiz, R.C., Kiatwuthinon, P., Kahn, J.S., Roh, Y.H., and Luo, D. (2012). Cell-free protein expression from DNA-based hydrogel (P-Gel) droplets for scale-up production. Ind. Biotechnol. *8*, 372–377.

32. Park, N., Um, S.H., Funabashi, H., Xu, J., and Luo, D. (2009). A cell-free protein-producing gel. Nat. Mater. *8*, 432–437. https://doi.org/10.1038/Nmat2419.

33. Emerson, M., Renwick, L., Tate, S., Rhind, S., Milne, E., Painter, H.A., Boyd, A.C., McLachlan, G., Griesenbach, U., Cheng, S.H., et al. (2003). Transfection efficiency and toxicity following delivery of naked plasmid DNA and cationic lipid-DNA complexes to ovine lung segments. Mol. Ther. *8*, 646–653. https://doi.org/10.1016/s1525-0016(03)00233-8.

34. Pardo, Y.A., Yancey, K.G., Rosenwasser, D.S., Bassen, D.M., Butcher, J.T., Sabin, J.E., Ma, M., Hamada, S., and Luo, D. (2022). Interfacing DNA hydrogels with ceramics for biofunctional architectural materials. Mater. Today *53*, 98–105. https://doi.org/10.1016/j.mattod.2021.10.029.

35. Song, J., Lee, M., Kim, T., Na, J., Jung, Y., Jung, G.Y., Kim, S., and Park, N. (2018). A RNA producing DNA hydrogel as a platform for a high performance RNA interference system. Nat. Commun. *9*, 4331–ARTN.4331. https://doi.org/10.1038/s41467-018-06864-0.

36. Jiao, Y., Liu, Y., Luo, D., Huck, W.T.S., and Yang, D. (2018). Microfluidic-assisted fabrication of clay microgels for cell-free protein synthesis. Acs Appl Mater Inter *10*, 29308–29313. https://doi.org/10.1021/acsami.8b09324.

37. Zhu, B., Gan, R., Cabezas, M.D., Kojima, T., Nicol, R., Jewett, M.C., and Nakano, H. (2020). Increasing cell-free gene expression yields from linear templates inEscherichia coliandVibrio natriegensextracts by using DNA-binding proteins. Biotechnol. Bioeng. *117*, 3849–3857. https://doi.org/10.1002/bit.27538.

38. Kim, H., Jeong, J., Kim, D., Kwak, G., Kim, S.H., and Lee, J.B. (2017). Bubbled RNA-based cargo for boosting RNA interference. Adv. Sci. *4*, 1600523. https://doi.org/10.1002/advs.201600523.

39. Kim, D., Kim, H., Lee, P.C.W., and Lee, J.B. (2020). Universally applicable RNA membrane-based microneedle system for transdermal drug delivery. Mater. Horiz. *7*, 1317–1326. https://doi.org/10.1039/C9MH01838G.

40. Liu, W.Q., Zhang, L., Chen, M., and Li, J. (2019). Cell-free protein synthesis: recent advances in bacterial extract sources and expanded applications. Biochem. Eng. J. *141*, 182–189. https://doi.org/10.1016/j.bej.2018.10.023.

41. Conway, J.W., McLaughlin, C.K., Castor, K.J., and Sleiman, H. (2013). DNA nanostructure serum stability: greater than the sum of its parts. Chem. Commun. *49*, 1172–1174. https://doi.org/10.1039/c2cc37556g.

42. Chandrasekaran, A.R. (2021). Nuclease resistance of DNA nanostructures. Nat. Rev. Chem *5*, 225–239. https://doi.org/10.1038/s41570-021-00251-y.

43. Lee, J.B., Hong, J., Bonner, D.K., Poon, Z., and Hammond, P.T. (2012). Self-assembled RNA interference microsponges for efficient siRNA delivery. Nat. Mater. *11*, 316–322. https://doi.org/10.1038/Nmat3253.

44. Han, S., Ko, O., Lee, G., Jeong, S.W., Choi, Y.J., and Lee, J.B. (2021). Rapid diagnosis of

coronavirus by RNA-directed RNA transcription using an engineered RNA-based platform. Nano Lett. *21*, 462–468. https://doi.org/10.1021/acs.nanolett.0c03917.

45. Yao, C., Tang, H., Wu, W., Tang, J., Guo, W., Luo, D., and Yang, D. (2020). Double rolling circle amplification generates physically cross-linked DNA network for stem cell fishing. J. Am. Chem. Soc. *142*, 3422–3429. https://doi.org/10.1021/jacs.9b11001.

46. Dahl, F., Banér, J., Gullberg, M., Mendel-Hartvig, M., Landegren, U., and Nilsson, M. (2004). Circle-to-circle amplification for precise and sensitive DNA analysis. Proc. Natl. Acad. Sci. USA *101*, 4548–4553. https://doi.org/10.1073/pnas.0400834101.

47. Nolan, T., Hands, R.E., and Bustin, S.A. (2006). Quantification of mRNA using real-time RT-PCR. Nat. Protoc. *1*, 1559–1582.

48. Cheatham, T.E., and Kollman, P.A. (1997). Molecular dynamics simulations highlight the structural differences among DNA:DNA, RNA:RNA, and DNA:RNA hybrid duplexes. J. Am. Chem. Soc. *119*, 4805–4825. https://doi.org/10.1021/ja963641w.

49. Xu, Y., Huang, K., Lopez, A., Xu, W., and Liu, J. (2019). Freezing promoted hybridization of very short DNA oligonucleotides. Chem. Commun. *55*, 10300–10303. https://doi.org/10.1039/C9CC04608A.

50. Le, Y., Chen, H., Zagursky, R., Wu, J.H.D., and Shao, W. (2013). Thermostable DNA ligase-mediated PCR production of circular plasmid (PPCP) and its application in directed evolution via in situ error-prone PCR. DNA Res. *20*, 375–382. https://doi.org/10.1093/dnares/dst016.

51. Edelheit, O., Hanukoglu, A., and Hanukoglu, I. (2009). Simple and efficient site-directed mutagenesis using two single-primer reactions in parallel to generate mutants for protein structure-function studies. BMC Biotechnol. *9*, 61. https://doi.org/10.1186/1472-6750-9-61.

STAR★ METHODS

KEY RESOURCES TABLE

REAGENT or RESOURCE	SOURCE	IDENTIFIER
Chemicals, peptides, and recombinant proteins		
Phi29 DNA polymerase	Lucigen	Cat# 30221-2
dNTP Mix (25 mM Mix)	Thermo scientific	Cat# R1122
Nuclease free water	IDT	Cat# 11-05-01-04
Sylgard	Sewinghightech	Cat# 184
GelRed® Nucleic Acid Gel Stain	Biotium	Cat# 41003
Critical commercial assays		
1-Step Human Coupled IVT Kit	Thermo scientific	Cat# 88881
High-Capacity RNA-to-cDNA Kit	Thermo scientific	Cat# 4387406
RNeasy Kits	Qiagen	Cat# 74104
TnT® Quick Coupled Transcription Kit	Promega	Cat# L1170
Beetle lysis-juice 2x	Takara	Cat# 102516
PowerUp™ SYBR™ Green Master Mix	Thermo scientific	Cat# A25742
Oligonucleotides		
pIDTSMART-AMP_EGFP	This paper	N/A
Primer 1 (GFP)	This paper	N/A
Primer 2 (T7)	This paper	N/A
VB211220-1262uwk_Luc	This paper	N/A
Primer 1 (Luc)	This paper	N/A
Primer 2 (T7)	This paper	N/A
Software and algorithms		
XEI 4.3.4	Park systems	https://park-systems-xei.software.informer.com/4.3/
Hitachi SU8000	Hitachi	https://www.hitachi-hightech.com/
CFX Maestro Software	Bio-rad	https://www.bio-rad.com/ko-kr/
RheoCompass	Anton Parr	https://www.anton-paar.com/
Image J	NIH	https://imagej.nih.gov/ij/
Image lab software	Bio-rad	https://www.bio-rad.com/ko-kr/product/image-lab-software?ID=KRE6P5E8Z
Graph pad prism 8 software	GraphPad Software	https://www.graphpad.com/scientific-software/prism/
SnapGene	SnapGene	https://www.snapgene.com/

RESOURCE AVAILABILITY

Lead contact

Further information and requests regarding resources and reagents should be directed to and will be fulfilled by the lead contact, Jong Bum Lee (jblee@uos.ac.kr).

Materials availability

- The plasmids utilized in this study were intentionally designed by the authors to fulfill specific requirements.
- All reagents generated in this study will be made available on request, but we may require a payment and/or a completed Materials Transfer Agreement if there is potential for commercial application.

Data and code availability

- All data reported in this article will be shared by the lead contact upon request.
- The software that was used in this study is listed in the key resources table.
- Any additional information required to analyze the data reported in this study will be made available by the lead contact upon request.

METHOD DETAILS

Synthesis of multimeric genomic DNA hydrogel

The plasmid hydrogel was designed using the Snapgene tool and purchased from Integrated DNA Technologies (IDT, IA, USA) and Vectorbulider (IL, USA) (Table S1 and S2). The synthesis of the plasmid hydrogel was carried out in three main steps with thermal cycler (T100, Bio-Rad, CA, USA). First, the double-stranded DNA plasmid (30 nM) was denatured to single-stranded DNA plasmid by heating it at 95°C for 5 min.[50,51] Second, two complementary single-stranded DNA plasmids, along with T7 primer (15 μM) and GFP primer (15 μM), were mixed in nuclease-free water and incubated at 50°C for 30 min, followed by slow cooling to 30°C for 10 min to allow annealing of the two complementary strands. Third, the DNA plasmid hydrogel was synthesized using reaction polymerase Ø29 (1.5 U/μL) at 30°C for 72 h in the presence of dNTPs (1.5 mM). The plasmid hydrogel was heated to 65°C for 10 min to inactivate the enzyme. Finally, the DNA plasmid hydrogel was gently washed thrice with nuclease-free water to remove any unreacted components.

AFM imaging

The AFM imaging was performed to analyze the mGD-gel at different time points, including 0.5, 2, 6, 12, and 24 h. To prepare the samples, they were diluted in AFM buffer containing 10 mM $MgCl_2$ and nuclease-free water. For analysis, 20 μL of the diluted sample was deposited on a freshly cleaved mica substrate with a DNA concentration of 0.5 to 1.0 ng/μL and incubated at room temperature (RT) for 5 min. Following incubation, the samples were rinsed with nuclease-free water and dried in a vacuum chamber. The AFM imaging was performed using a Park Systems NX10 in non-contact mode with a PPP-NCHR probe. The images were flattened using the XEI 4.3.4 program (Park Systems, CA, USA).

Rheological test

The rheological properties of the mGD-gel were analyzed using a controlled stress rotational rheometer MCR302 (Anton Par, VA, USA) at room temperature (25°C). A plate-plate geometry with a 25 mm diameter parallel plate and a gap size of 1 mm was used to measure the mechanical properties. The dynamic shear strain sweep test was performed by applying a range of 0.01 % to 10 % strain with a fixed frequency of 10 rad/s. The dynamic frequency sweep test was carried out by applying a range of 0.1 rad/s to 10 rad/s with a fixed strain of 0.05 %.

Green fluorescent protein quantification

The quantification of protein expression in the mGD-hydrogel was carried out using a gel imaging system (Bio-Rad, CA, USA) equipped with a blue tray (Bio-Rad, CA, USA) using by GelDoc (Gel Doc™ EZ System, Bio-Rad, CA, USA). Protein expression quantification analysis was performed using a 1-step *in vitro* transcription and translation (IVT) human coupled kit (Thermo Fisher Scientific, MA, USA). The quantification of green fluorescent protein (GFP) production was carried out using real-time polymerase chain reaction with excitation at 489 nm and emission at 511 nm. The assay was conducted following the manufacturer's instructions: 1) The mGD-hydrogel was mixed with HeLa lysate, accessory proteins, reaction mix, and nuclease-free water. 2) The mixture was then incubated at 30 °C. 3) GFP fluorescence values were measured at 3 h intervals for 96 h using the real-time PCR (CFX-96, Bio-Rad, CA, USA).

Analysis of Luciferase protein quantification

Analysis of Luciferase protein quantification was performed using the TnT® Quick Coupled Transcription Kit (Promega, WI, USA). The experiment was conducted following the protocol provided in the kit. Firstly, the Luc-mGD-gel was incubated with master mix and methionine at 30°C. Next, Beetle lysis-juice 2x (Takara, Japan) was added to the mixture with the gel, and then incubated for 10 min at room temperature. Luminescence was subsequently analyzed in a 96-well white plate using a plate reader (The Synergy™ 2, BioTeK, VT, USA).

GFP mRNA level quantification

The *in vitro* translation mixtures were first treated with DNase I for 5 min to remove any remaining plasmid DNAs or amplified DNAs. Then, the transcribed RNAs were extracted from the same volume of mixtures using RNA extraction kits (RNeasy Kits, Qiagen, Hilden, Germany), according to the manufacturer's protocols. RNA content was measured using a UV-Vis spectrophotometer (NanoDrop 2000c, Thermo Fisher Scientific, MA, USA), and cDNA was synthesized using a High-Capacity RNA-to-cDNA kit (Applied Biosystems™, MA, USA) according to the manufacturer's protocol. Finally, cDNAs were amplified using Taq DNA polymerase enzyme (PowerUp™ SYBR™ Green Master Mix, Applied Biosystems™), and the extent of amplification was measured using StepOnePlus Real-Time PCR System (Applied Biosystems™, MA, USA).

Freeze-casting

The mGD-gel fit in the PDMS molds. For freezing, molds with mGD-gel incubated for 15 min at -80°C with deep freezer (UniFreeze TM, Daihan Scientific, Korea). Next, to cast the mGD-gel in the mold, the mold was alternately twisted and transferred to nuclease-free water.

QUANTIFICATION AND STATISTICAL ANALYSIS

All data were analyzed using the GraphPad Prism 8 software package (GraphPad Software, CA, USA). All groups were compared using Student's t-test or one-way ANOVA, and a value of $p < 0.05$ was considered statistically significant.